

# TOMOGRAPHIC INVERSIONS IN SHALLOW WATER, USING MODAL TRAVEL TIME MEASUREMENTS

Michael I. Taroudakis and Maria Markaki,

University of Crete, 714 09 , Heraklion Crete, HELLAS

e-mail: [taroud@iacm.forth.gr](mailto:taroud@iacm.forth.gr)

and

Foundation for Research and Technology-Hellas, Institute of Applied and  
Computational Mathematics, P.O.Box 1527, 711 10 Heraklion, Crete, HELLAS.

**Abstract-** The paper deals with an inversion approach based on modal travel time measurements for the estimation of water column and bottom properties in shallow water, by acoustic means. The modal structure of the acoustic field measured at a single hydrophone is defined on the basis of group velocity predictions at the central frequency of a broadband signal (tomographic signal). In the proposed approach, the assumption of good a-priori knowledge of the parameters to be recovered which is normally applied in modal-travel time inversion schemes, is waived and a relatively wide search space is considered. Following an identification process to assign modal arrivals to the peaks of the measured signal, a matching procedure is adopted based on the minimization of a cost function relating the travel time differences of the identified peaks with respect to the modal travel times for the same peaks. This procedure leads to a set of environments, which are considered close to the actual one, among which a reference environment for the application of a linear inversion procedure is chosen on the basis of the convergence of the local search. Thus, the inversion procedure adopted is hybrid in the sense that an optimization procedure for the estimation of the most probable reference environment is combined with a linear inversion method to estimate the unknown parameters. The approach can be applied in shallow water tomographic experiments involving a single source-receiver pair and leads to the simultaneous estimation of water and sediment sound velocities.

## 1. Introduction

The paper presents an acoustical inversion technique for the estimation of environmental parameters in shallow water based on the identification of the modal structure of a broad-band signal measured at a single hydrophone. The motivation for the work presented here is based on the limitations of conventional approaches for geoacoustic inversion. For instance, if a wide search space is the only a-priori information on the parameters to be recovered, linear methods based on modal travel time information [1,2] fail, unless a background environment close to the actual one is defined. On the other hand, ray methods in shallow water when applied with long range data may be not appropriate due to the fact that the acoustic field for this case is characterized by its modal structure. Still, broad-band matched-field methods using the whole arrival pattern shape as their observable, have the disadvantage that as they have to handle noisy data in the real world, the actual amplitude of the signal at a single receiver under low signal to noise ratio cannot be treated with enough reliability.

An alternative would be to look for observables that are not affected greatly by noise. Modal arrivals seem to be the solution to this problem as their location in the time

history of the signal is rather stable and if their amplitudes are above a certain threshold, they can in principle be identified. Of course source-receiver separation has to be large enough so that the modal arrivals are well-resolved [2]. In most cases of interest the identification of a certain number of modal arrivals is possible with acceptable reliability

The inversion scheme proposed here combines an optimisation procedure based on the minimization of an appropriate cost function, and a modal identification procedure, which is necessary in order to determine the observables and define the cost function. An additive feature of the method is that it can be viewed as a "background" environment provider for the application of a linear inversion scheme rather than a solver to the inverse problem. When the linear inversion procedure is added, the whole scheme is characterized as "hybrid" combining non-linear and linear approaches to the inverse problem in a way very similar to the one presented in [3].

Although the method can be applied for multidimensional inversions including water and bottom parameters simultaneously, inversion results presented here are referred to the recovery of water and bottom parameters separately. The bottom parameter to be recovered is the sound speed profile in the first sediment layer, as this parameter is considered to be the most important for sediment classification and, as several works have shown, the one that affects most the acoustic field in water.

The structure of the paper is as following: Section 2 presents the forward problem. The inverse problem is defined in section 3. The proposed inversion procedure is presented in section 4. The application of the proposed method in selected environments is presented in section 5 and the conclusions from the application of the method are discussed in section 6.

## 2. The forward problem

We will consider acoustic propagation in an oceanic range-independent waveguide. The acoustic pressure  $P(\vec{x})$  due to a monochromatic source of frequency  $f$  and unit strength is governed by the Helmholtz equation. The forward propagation problem concerns the calculation of the acoustic field at a specific circular frequency  $\omega = 2\pi f$ , when the environmental parameters that includes water column and bottom properties are known:

$$\nabla^2 P(\vec{x}) + k(\vec{x})^2 P(\vec{x}) = -\delta(\vec{x} - \vec{x}_0) \quad (1)$$

The equation is supplemented by the appropriate boundary and interface conditions and a Sommerfeld radiation condition for the behaviour of the field at infinity, to form a well-posed problem in the sense that there exists a single solution to it. Here,  $k$  is the wavenumber ( $k = \omega / c$ ),  $\vec{x}$  is the position vector of the receiver and  $\vec{x}_0$  is the position vector of the source. Note that  $P(\vec{x})$  thus defined is actually the system transfer function  $H(\omega)$  of the oceanic waveguide when the latter is considered as a linear system [4].

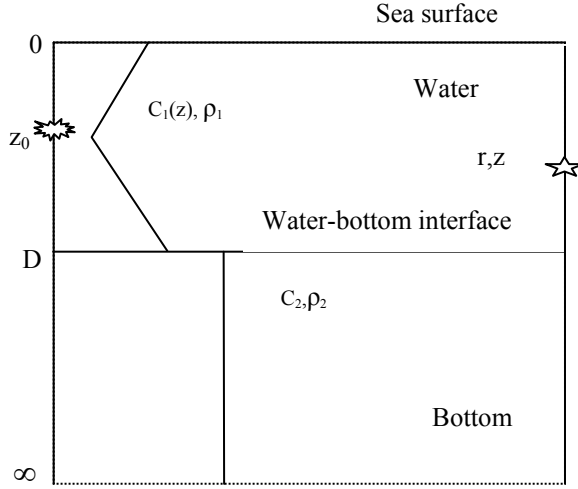


Figure 1. The oceanic waveguide with a semi-infinite bottom

We will restrict our analysis to the normal-mode solution of the problem in an axially symmetric range-independent environment for which a cylindrical co-ordinate system is considered. The acoustic pressure is expressed by means of an eigenfunction expansion in the form:

$$\begin{aligned}
 P(r, z) &= \sum_{n=1}^N A_n(r) u_n(z) = \\
 &= \frac{e^{i\frac{\pi}{4}}}{\sqrt{8\pi\rho(z_0)}} \sum_{n=1}^N \frac{u_n(z_0) u_n(z)}{\sqrt{k_n r}} e^{ik_n r} = \sum_{n=1}^N P_n(r, z)
 \end{aligned} \tag{2}$$

Here,  $k_n$  is the eigenvalue of order  $n$ ,  $u_n(z)$  is the associated eigenfunction of the "depth" problem defined below,  $\rho(z)$  is the density, considered constant in each layer and we have assumed that we are far away from the source, so that asymptotic expressions for the Hankel function involved in the expression of  $A_n(r)$  are valid [5].

$P_n(r, z)$  is the propagation mode of order  $n$ . Thus, the summation in (2) is extended over the  $N$  propagating modes, which for the case of a waveguide consisting of a water column (layer 1) and a semi-infinite fluid bottom (layer 2) as in figure 1 is determined by the discrete spectrum of the "depth" problem, which is actually a singular Sturm-Liouville problem:

$$\frac{d^2 u_n(z)}{dz^2} + (k(z)^2 - k_n^2) u_n(z) = 0 \tag{3}$$

where,

$$\begin{aligned}
 u_n(z) &= u_{1,n}(z), \quad 0 \leq z \leq D \\
 u_n(z) &= u_{2,n}(z), \quad D < z < \infty
 \end{aligned}$$

and

$$\begin{aligned}
 u_{1,n}(0) &= 0 \\
 u_{1,n}(D) &= u_{2,n}(D) \\
 \frac{1}{\rho_1} \frac{du_{1,n}}{dz}(D) &= \frac{1}{\rho_2} \frac{du_{2,n}}{dz}(D) \\
 \lim_{z \rightarrow \infty} u_{2,n}(z) &= 0
 \end{aligned}$$

If more than one interface exist, there is an analogous definition with multiple layers to be associated with related indices. The semi-infinite lower layer in the bottom is called "sub-bottom". The environmental parameters define the geometry of the interfaces and include the sound speed and the densities of the various layers  $c_i, \rho_i$ .

When the environmental parameters are known, the pressure field is uniquely defined (forward problem). If on the other hand measurements of the acoustic field for a specific experimental geometry are available, we can make use of them for the recovery of the environmental parameters in the water column and the bottom, defining corresponding classes of inverse problems which, as it is well known, are generally ill-posed problems.

Of particular interest are the problems of estimating the water parameters (practically the sound speed profile), or the bottom structure. Inverting for the bottom structure we are looking for the sound speed and densities in the various layers and for the location of the corresponding interfaces.

The experimental configuration and the type of existing measurements dictate the inversion method to be applied. When there is only a single hydrophone available for the measurement of the acoustic field, the problem is treated in the time domain. Normally a broad-band source is considered, characterized by its source excitation function  $S(\omega)$  (considered known). Using the solution for the pressure field due to a monochromatic source of unit amplitude and frequency  $\omega$  given in (2), we obtain an expression of the form:

$$p(r, z; \omega) = P(r, z; \omega) S(\omega) \quad (4)$$

written as:

$$p(r, z; \omega) = \sum_{n=1}^N P_n(r, z; \omega) S(\omega) \quad (5)$$

The treatment of the problem in the time domain can be done directly by solving the linearized acoustic wave equation in the time domain or alternatively by applying an inverse Fourier transform to the pressure field of the monochromatic source, to obtain:

$$p(r, z; t) = \mathfrak{F}^{-1}[p(r, z; \omega)]; \omega \rightarrow t = \frac{1}{2\pi} \int_{-\infty}^{\infty} \sum_{n=1}^N P_n(r, z; \omega) S(\omega) e^{i\omega t} d\omega = \sum_{n=1}^N \tilde{p}_n(r, z; t)$$

(6)

Each one of the terms in the sum corresponds to an energy packet associated with a specific mode order  $n$ .

The modal packets propagate at the group velocity defined as

$$v_{g,n} = \left. \frac{\partial \omega}{\partial k_n} \right|_{\omega_0} \quad (7)$$

An alternative expression using the eigenfunctions  $u_n$  is:

$$v_{g,n} = \frac{1}{c_n} \left( \int_0^\infty \frac{1}{\rho(z)} c^2(z) u_n^2(z) dz \right)^{-1} \quad (8)$$

where  $c_n = \omega / k_n$  is the phase velocity [6].

The arrival time of a modal packet at range  $r$  is simply

$$t_n = \frac{r}{v_{g,n}} \quad (9)$$

Note that not all the modal packets are resolvable in the time domain. For a complete discussion on mode resolvability see Munk [7]. Here it suffices to point out that modal packets are well resolved if the channel is not highly dispersive for the corresponding mode and if the group velocities of the adjacent modes differ by an adequate amount. [2], [8].

### 3. The inverse problem

Consider an environment where the arrival pattern, that is the magnitude of the signal measured in the time domain, consists of several peaks. These peaks can be described as either

1. Ray arrivals
2. Modal arrivals, or
3. Local maxima of the arrival pattern

The location of the peaks can be used for the classification of the environment because their corresponding travel times depend on the environmental parameters. Traditional ocean acoustic tomography is based on the ray arrivals and the peaks of the signal are associated with specific rays. [9]. Modal travel time tomography on the other hand is based on modal arrivals as they have been defined in the previous section [10]. First approaches in both cases were based on a perturbation analysis: A reference environment is defined and ray or modal travel times are calculated. Then the differences of the actual arrival times with respect to those calculated for the reference environment are derived. As these travel time differences depend, under a

functional relationship, on the differences of the actual environmental parameters with respect to those of the reference environment, a linear inverse problem is defined. In both cases ray or mode identification is assumed. The identification and tracking of the ray or modal arrivals is based on an appropriate procedure. The recoverable parameter is normally the sound speed profile. The use of empirical orthogonal functions simplifies the approach. [11]. Recently similar approaches based on the characterization of the peaks as local maxima of the signal have been developed with good results [12,13].

In all these cases a reference environment close to the actual one is assumed.. However this information may not be known in all practical applications. Instead a generally wide search space may be the only a priori knowledge for the unknown parameters. Thus, linear inversion schemes may not be appropriate despite the fact that suitable adaptive schemes have shown good performance [14].

An alternative way to proceed is to "match" the peaks of the actual pattern with those corresponding to a class of "candidate" environments, using an appropriate optimization criterion. This approach is analogous to the well established matched-field processing where an appropriate objective function forms the basis for the comparison of the actual acoustic field with the one corresponding to a candidate environment [15].

In the case of matched-field processing the observables are normally measurements of the acoustic pressure at a single range and several hydrophone locations,  $z_i, i = 1, \dots, I$ . (vertical array of hydrophones) for one ( $\omega$ ) or more ( $\omega_j, j = 1, \dots, J$ ) frequencies.

$$p_i(\omega_j) = p(r, z_i; \omega_j) \quad i = 1, \dots, I, \quad j = 1, \dots, J.$$

Alternatively one could use a horizontal array of hydrophones in which case the measurement positions correspond to different ranges  $r_i$

In our case, the observables are peaks of the magnitude of a broad-band signal (arrival pattern) measured at a specific location ( $r, z$ ).

$$\tilde{t}_i \rightarrow \frac{\partial |p(r, z; t)|}{\partial t} = 0 \quad i = 1, \dots, I$$

The expression above indicates that by following the local maxima of the maximum one defines  $I$  arrival times.

In both cases the observables form a vector, denoted as  $\mathbf{d} = [d_1, d_2, \dots, d_M]^T$ ,  $M = I$  (or  $I \times J$  if multi-depth multi-tone data are available in Matched field processing), associated with the recoverable parameters  $\mathbf{m} = [m_1, m_2, \dots, m_L]^T$ , where  $L$  is the number of parameters, through a non-linear matrix equation of the form

$$\mathbf{f}(\mathbf{d}, \mathbf{m}) = 0 \tag{10}$$

Note that this formulation implies discrete inverse theory and the recoverable parameters are treated as discrete values and not continuous functions of space.

The matched-field processing inversion is based on an optimization procedure to solve the non-linear equation above. The heart of the procedure is the objective function, which associates measurements with calculated replicas of the field for a set of candidate environments. The objective function is normalized so that its maximum value is 1 corresponding to perfect match.

In our approach the modal arrivals must be first identified before applying the model based inversions. This issue is a basic problem that is not present in conventional Matched-Field processing for instance. Indeed in travel time inversion problems, the observables of the actual and the candidate field do not necessarily correspond to each other. In order that an equation of the form (10) be valid, the peaks of the arrival pattern should characterize the same energy content. That is the peaks should characterize the same ray or modal packet or local maximum of the propagating energy (significant peaks). Thus, an identification process should precede any attempt to match the locations of the significant peaks of the actual and the estimated arrival pattern of the signal.

Here, we restrict our analysis to **modal arrivals** only, and propose an approach for handling the inverse problem based on a simultaneous identification and matching procedure of the modal arrivals as described below.

#### 4. The inversion procedure

The proposed approach can in principle be applied in cases where a multidimensional search space should be examined, that is, in cases where there are many model parameters to be recovered. However, the cases to be studied here and the specific procedure to be followed will be restricted to the recovery of the sound speed at the top and the bottom of the water and/or the sediment layer. A linear variation of the sound speed will be assumed between the top and the bottom of the corresponding layers (Figure 2). A sub-bottom of known parameters starting at depth  $D+h$  will also be assumed. Thus, the data vector will be  $\mathbf{d} = [c_{w,u}, c_{w,l}, c_{b,u}, c_{b,l}]^T$  when the sound speed in the water and bottom are to be recovered simultaneously and  $\mathbf{d}_w = [c_{w,u}, c_{w,l}]^T$  or  $\mathbf{d}_b = [c_{b,u}, c_{b,l}]^T$  when the two properties are to be estimated separately. Here the subscript  $w$  denotes water and  $b$  sediment, and  $u$  denotes upper and  $l$  lower.  $D$  and  $h$  will be considered fixed.

According to the geometry presented in Figure 2,  $c_{w,u} = c_w(0)$ ,  $c_{w,l} = c_w(D)$ ,  $c_{b,u} = c_b(D)$ ,  $c_{b,l} = c_b(D+h)$

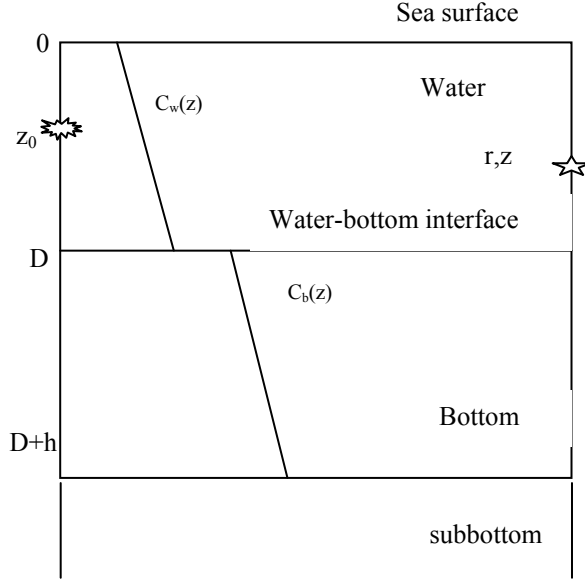


Figure 2. The oceanic waveguide. The inversion scheme recovers the sound speed profiles  $c_w(z)$  and  $c_b(z)$ . Measurements are made at range  $r$  and depth  $z$ .

#### 4.1 Discretization of the search space

We will assume a search space for each one of the recoverable parameters and we discretize it so that a number of candidate environments is defined. For simplicity we will consider separately the problems of water and bottom sound speed recovery. Thus two-dimensional search spaces are defined in each case.

Note that the application of this procedure in multidimensional inversion cases is more complicated and time consuming taking into account the great number of candidate environments that should be examined. For these cases, the simple grid search algorithm adopted here should be replaced by more sophisticated search algorithms such as those based on Simulated Annealing [16], Genetic Algorithms [17],[18],[19] or others [20],[21], possibly incorporating a posterior statistical analysis for the presentation of the results as in [18].

To perform the search in our case we define  $K_p = K \times P$  environments corresponding to a pair of parameters  $(c_{*,u,k}, c_{*,l,p})$ ,  $k = 1, \dots, K$   $p = 1, \dots, P$  and  $*$  stands for  $w$  or  $b$  according to the specific problem in hand.

For each one of the pairs thus defined, an identification algorithm is applied to associate the potential modal peaks of the signal with the actual peaks of the measured arrival pattern. The algorithm has been presented in [22] for a single reference environment and is briefly described in the next subsection.



## 4.2 The identification algorithm

The identification of the peaks of the measured signal that correspond to modal arrivals is done on the basis of the "reference environment" which is considered known. The reference environment coincides with the candidate environment defined above. The arrival times of the modal peaks of this environment are simply defined using calculations of the group velocity at the central frequency. Actually the identification process is the first stage of an inversion toolbox prepared to treat tomographic signals in the time domain for general inversions.

As mentioned before, the absolute value of a broad-band signal recorded in the receiver (arrival pattern) contains  $I$  peaks characterized as local maxima of the magnitude of the field :

$$\tilde{t}_i \rightarrow \frac{\partial |p(r, z; t)|}{\partial t} = 0 \quad i = 1, \dots, I \quad (11)$$

Some of these peaks are characterized as modal arrivals (peaks) in the sense that they correspond to the modal packets. For these peaks  $\tilde{t}_i = t_j$ , for some  $j$  where  $j = 1, \dots, \tilde{N}$ .  $t_j$  is the travel time of the  $j$ th mode and  $\tilde{N}$  is the highest order of propagating modes.

For the peaks in the reference environment denoted by  $\tilde{t}_i^0$  and corresponding to the pair  $(c_{*,u,k}, c_{*,l,p})$  we have :

$$\tilde{t}_i^0 \rightarrow \frac{\partial |p^0(r, z; t)|}{\partial t} = 0 \quad i = 1, \dots, I^0 \quad (12)$$

where  $I^0$  is not necessarily equal to  $I$ .

The peaks corresponding to the modal packets are the peaks for which  $\tilde{t}_i^0 = t_j^0$   $j = 1, \dots, N$ , where  $N$  is the highest order of propagating modes in the reference environment.

Note that  $\tilde{N}$  may be different from  $N$ . Thus, by setting  $M = \min\{N, \tilde{N}\}$  we will restrict our analysis to  $M$  modes.

Letting  $\delta t_{ij} = \tilde{t}_i - t_j^0$  be the difference between the arrival times of the peaks of the actual signal and the modal arrivals of the reference environment and assuming that the modal arrivals of the actual field appear in locations close to those of the reference one, we search among all possible pairs for the  $\delta t_{ij}$  which is minimum. By repeated application of this procedure and imposing a threshold for the amplitude of the identified peaks (low amplitude peaks may be due to noise and therefore should be excluded from the identification), we obtain a set of identified modal peaks.

Note that unless a perfect match between modal travel times of the reference environment and peaks of the measured arrival pattern is achieved, a vector consisting of the elements  $\delta t_{i(k,p)}$ ,  $i = 1, \dots, \hat{M}_{k,p}$  of the time differences between the estimated and the actual modal arrival times for the identified peaks is defined. Here  $\hat{M}_{k,p}$  is the number of identified modal peaks for the actual arrival pattern based on the reference environment corresponding to the pair  $(c_{*,u,k}, c_{*,l,p})$ .

The advantage of this identification approach is that it is easily applied, since it is only the modal velocity of the reference environment for the central frequency, which needs to be calculated. Thus, the identification process is very fast and there is no need to calculate the field in the time domain for the reference stage.

The procedure is repeated for all sets of candidate reference environments.

It should be noted here, that the identified modal peaks are not necessarily correct ! This is due to the fact that the identification approach is based on the assumption that the reference environment is close to the actual one, which is not necessarily the case, with the exception of a sub-set corresponding to an area close to the true solution. Therefore some local peaks could be treated as modal arrivals only because they appear at a time corresponding to the arrival time of a specific modal packet. As the amplitude of the peak is not taken into account (it is considered not reliable) there is no second check to avoid this misinterpretation

#### 4.3 Optimization

Using the identification approach described above, we have defined  $\hat{M}_{k,p}$  vectors of travel time differences between identified modal arrivals and corresponding modal travel times for the reference environments. A direct way to proceed is to calculate for all these vectors the norm

$$P_{k,p}(\delta t_{i(k,p)}) = \sqrt{\frac{1}{\hat{M}_{k,p}} \sum_{i=1}^{\hat{M}_{k,p}} \delta t_{i(k,p)}^2} \quad (13)$$

and choose among all reference environments the one which corresponds to minimum norm. This approach does not take into account the absolute number of identified modal arrivals and may result to the selection of a reference environment, which is not the closest to the actual one.

A direct alternative is to choose the environment corresponding to the minimum norm among the environments for which a maximum number of modal arrivals have been identified. This is considered safer than the previous method, as one would expect the environment closest to the actual one to provide the maximum number of identified modal arrivals.

It should be noted that this approach is deterministic in the sense that no statistical analysis of the most probable reference environment is applied. If the idea is to be

applied in multidimensional cases, the a-posteriori statistical analysis following a sophisticated search algorithm would be preferable.

#### 4.4 Local search.

The procedure described above is terminated by assigning a reference environment which, when used in connection with an identification scheme, associates the maximum number of modal peaks with the peaks of the arrival pattern of the actual signal and the corresponding norm defined in (13) takes the minimum value. In theory, this environment is considered very close to the actual one and the inversion procedure could stop here. However a local search is expected to improve the results and lead the algorithm to an environment closest to the actual one. This can be achieved by different ways. One alternative is to repeat the search described above with a finer grid. Another alternative is to apply a linear inversion scheme based on a perturbation approach as described in [10] or [11]. We will proceed here adopting the second alternative.

A relationship between travel time and sound speed differences is derived using group velocity considerations, leading to the formula :

$$\delta t_n = t_n - t_n^0 = \frac{\partial \delta k_n r}{\partial \omega} = \frac{\partial}{\partial \omega} \left( \frac{r}{k_n^0} \int_0^\infty \frac{1}{\rho(z)} |u_n^0(z)|^2 \frac{k^{02} \delta c(z)}{c_0(z)} dz \right) \quad (14)$$

where index 0 denote quantities referred to the reference environment and  $n$  is the order of the corresponding mode.

The sound speed difference is defined as

$$\delta c(z) = c(z) - c_0(z) \quad (15)$$

Thus a vector on the travel time differences for the identified modal arrivals is defined:

$$\delta \mathbf{t} = [\delta t_1, \delta t_2, \dots, \delta t_i, \dots, \delta t_M]^T$$

where  $M$  is the number of identified peaks for the reference environment. Of course  $M = M_{k,p}$  for  $(k, p)$  corresponding to the reference environment chosen as the basis for the local search.

The continuation depends on the availability of the a-priori knowledge of the sound speed variation with respect to depth. Arbitrary variation dictates the discretization of the environment in small segments in depth, within each of which the velocity remains constant. Thus a vector of the unknown values of the sound speed differences in the segments is determined for  $L$  segments in depth:

$$\delta \mathbf{c} = [\delta c_1, \delta c_2, \dots, \delta c_l, \dots, \delta c_L]^T$$

The inversion scheme searches for these values and results in a linear system of equations of the form:

$$\delta \mathbf{t} = \mathbf{Q}_0 \delta \mathbf{c} \quad (16)$$

The kernel  $\mathbf{Q}_0$  as seen from (14) is defined by the properties of the reference environment.

Another possibility is to express the sound speed variation in terms of empirical orthogonal functions (EOF's):

$$\delta c(z) = \sum_{k=1}^K A_k \phi_k(z) \quad (17)$$

Then, a similar form for the unknown amplitudes of the EOF's can be defined [11].

$$\delta \mathbf{t} = \hat{\mathbf{Q}}_0 \delta \mathbf{a} \quad (18)$$

where,

$$\delta \mathbf{a} = [A_1, A_2, \dots, A_K]^T$$

Note that the vector of the travel time differences  $\delta \mathbf{t}$  has already been defined using the identification procedure

When a linear variation with depth is assumed, and the water depth and sediment thickness is known, the appropriate EOF's are defined as following:

$$\varphi_{1w}(z) = z, \quad \varphi_{2w}(z) = \frac{2 * D}{3} - z \quad (19a)$$

and

$$\varphi_{1b}(z) = z, \quad \varphi_{2b}(z) = \frac{2 * h}{3} - z \quad (19b)$$

where,  $w$  is referred again to the water column of depth  $D$  and  $b$  to the sediment layer of thickness  $h$  respectively.

The sound speed differences with respect to a constant or linearly varying reference sound speed are expressed in the form

$$\delta c_w = a_1 \varphi_{1w} + a_2 \varphi_{2w} \quad (20a)$$

and

$$\delta c_b = b_1 \varphi_{1b} + b_2 \varphi_{2b} \quad (20b)$$

By substituting expressions (20a,b) in (14), we come-up with a linear system of equations of the form (18) with respect to the four unknowns  $a_1$ ,  $a_2$ ,  $b_1$ , and  $b_2$  when there is a simultaneous recovery of the water and bottom properties, or with

respect to two unknowns  $(a_1, a_2)$  or  $(b_1, b_2)$  when the two problems are treated separately.

We will not discuss the properties of the system here. It suffices to say that it may be over-determined if the number of equations, which is related to the number of identified modes, is more than 4 (or 2). Such a system may be solved for instance by means of a Singular Value Decomposition algorithm [4].

A subject under investigation is the convergence of an iterative algorithm based on the linear approach, according to which the environment recovered in each one of the iterations is considered as the background for the next iteration. The procedure is considered convergent if it generates an environment, which differs very little with respect to the background one, the difference measured through an appropriate norm.

Extensive computational effort has shown that the procedure converges when the reference environment is indeed close to the actual one. This provides us with an additional check of the reliability of the reference environment determined through the matching procedure. If the reference environment is not close to the actual one, the iterative procedure is not expected to converge. The convergence properties of the iterative scheme are though a subject of current research.

Note that in the application of the iterative procedure there are two options with regard to the identified peaks. As the reference environment determined in each step is different from the one in the previous step, there is a possibility of performing a new identification at each step of the iteration. Alternatively, it is possible to keep the identified modal arrivals according to the original assignment of the reference environment.

In the applications to follow we will adopt the second option for simplicity. Thus there is a substantial saving in the execution time.

The whole procedure is described as flowcharts in Figures 3 and 4 and it is realized with the help of a toolbox developed at FORTH. The input of the toolbox is the tomographic signal measured in the time domain. Normally the input signal is the average of several receptions. The search bound is another set of input values for the toolbox. The output comes in two stages. The output of the first stage is a set of reference environments defined through the matching procedure and corresponding to the maximum number of identified peaks. The number of the elements in the set depends on the criteria imposed in the matching procedure. The input of the second stage corresponding to the linear inversion scheme is the set of reference environments defined in the first stage. A single sound speed profile is the outcome of the second stage, provided that the linear inversion scheme converges.

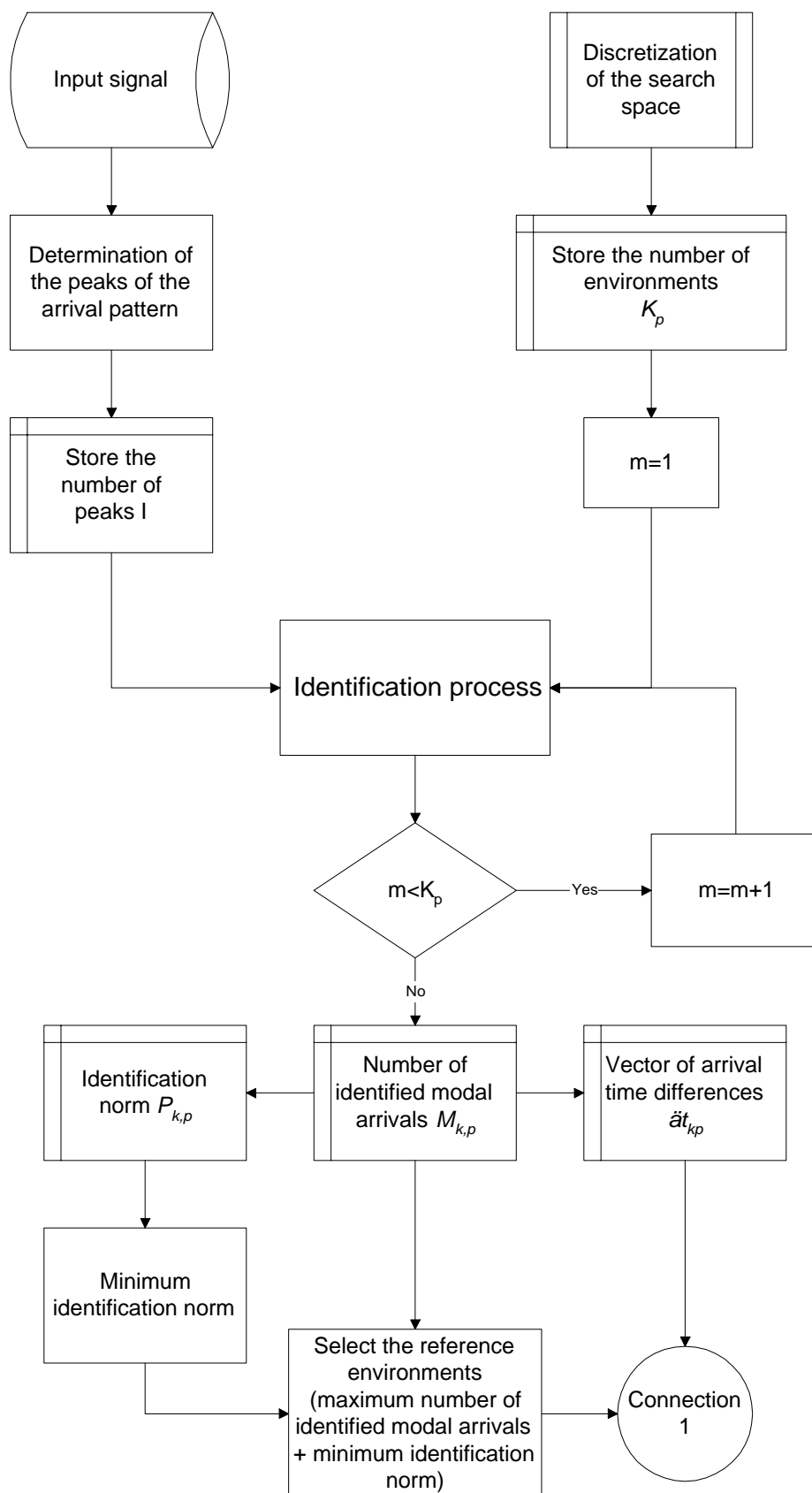


Figure 3 The matching procedure

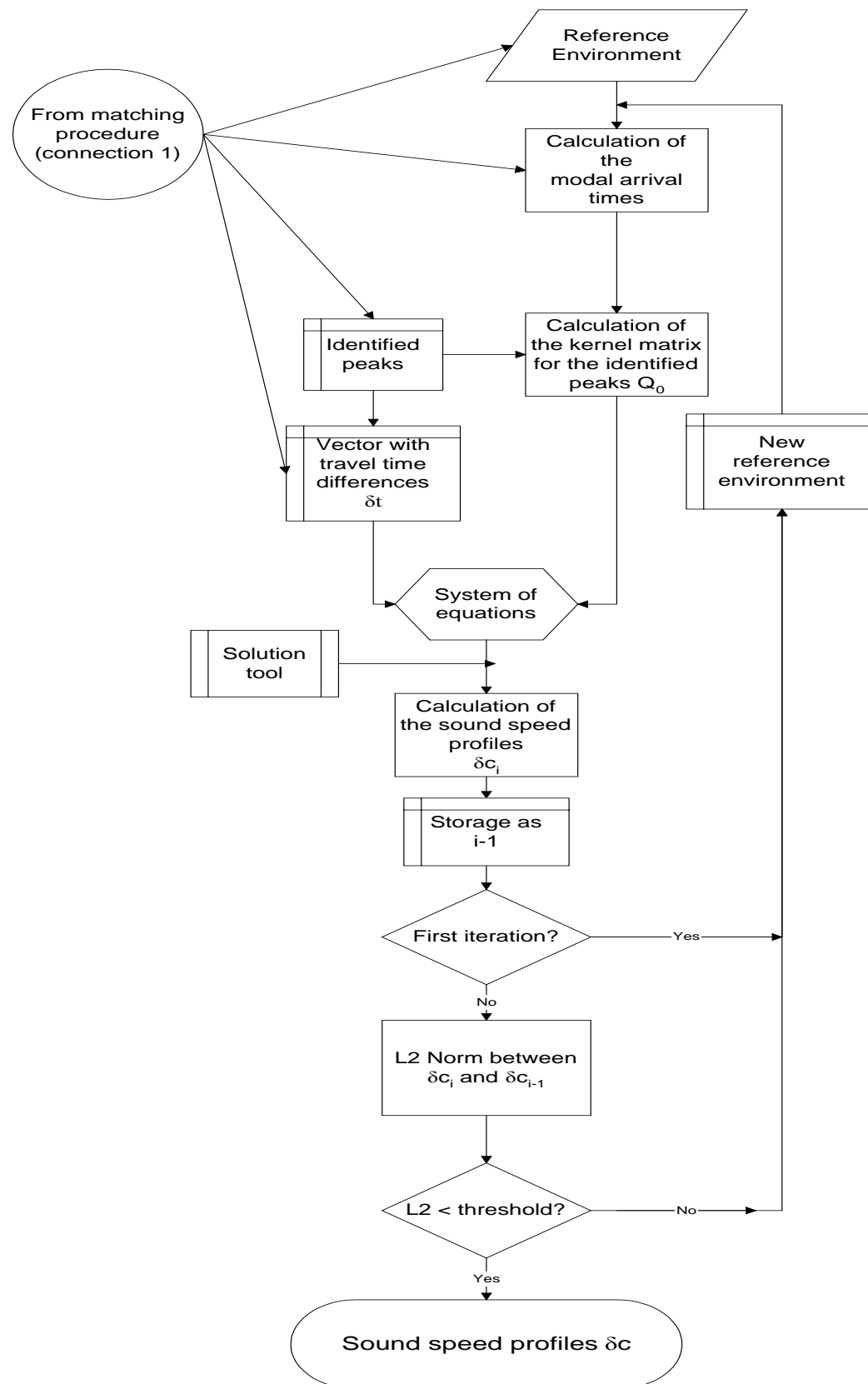


Figure 4. The iterative linear procedure

#### 4.5 Using the approach for bottom recovery

In theory the proposed approach seems to work well for water and bottom sound speed recovery. However since the information on the bottom structure contained in a specific mode is related to the amount of bottom penetration of the mode, it is reasonable to expect that higher order modes penetrating deeper in the bottom are preferable for bottom identification. At the same time it is generally understood that higher order modes are more difficult to identify. Therefore it is expected that the better the identification of the higher order modes, the better is the quality of bottom recognition.

### 5. Illustrative application examples

#### 5.1 The environment of the test case

The proposed approach will be applied for bottom and water sound speed inversion using synthetic data from a characteristic benchmark exercise designed to test bottom geoacoustic inversion algorithms [23]. Synthetic data at various frequencies and receiving locations corresponding to the environment presented in figure 5 were available to the participants. In our case we have chosen to use the data for the recovery of the sound speed profile in the sediment layer (considering the actual sediment thickness and the characteristics of the sub-bottom known) or of the sound speed profile in water (considering all of the bottom properties known). The water depth and the location of the sound source are also considered known. Additional information exploited in our inversion scheme is the fact that the sound speed profiles in water and sediment layer changes linearly with depth.

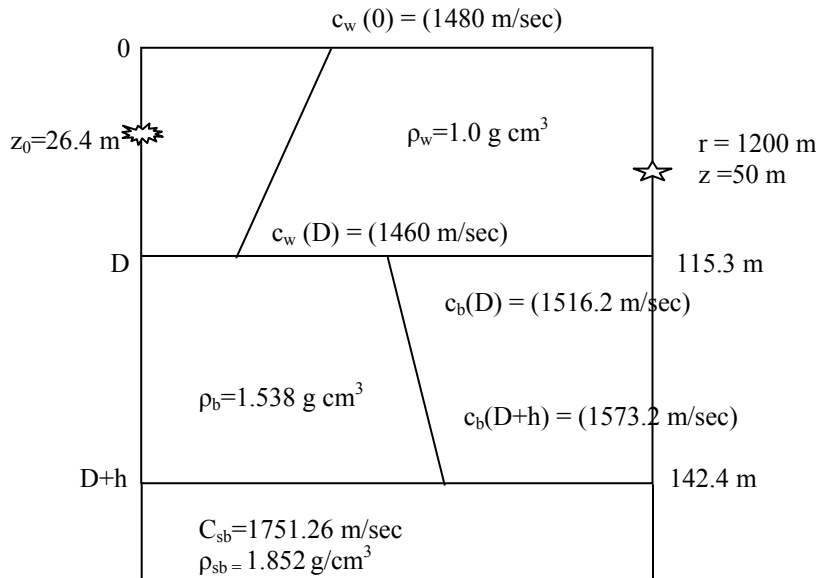


Figure 5. The environment of the test case.



We have used the data available as complex pressure values at a distance of 1200 m from the source and a depth 50 m to represent the actual measurements  $p(\omega_i)$ ,  $i=1,\dots,N_1$  where  $N_1$  was the number of available data points. In our case  $N_1$  was equal to 200. Taking into account that usual tomographic sources can be modelled in the frequency domain using a gaussian function to represent the source excitation function  $S(\omega)$ , we passed a gaussian filter of central frequency  $f_0=115$  Hz and bandwidth  $\Delta f=50$  Hz over the available data to simulate the spectrum of the measured signal.

Thus, the input to the discrete inverse Fourier transform applied for getting the signal in the time domain is

$$p(r, z; \omega_i) = P(r, z; \omega_i) S(\omega_i), \quad i=1, \dots, N_1 \quad (21)$$

where

$$S(\omega_i) = \exp\left\{-\frac{(\omega_i - \omega_0)^2 4\pi}{(\Delta\omega)^2}\right\} \quad (22)$$

The output of the discrete inverse Fourier transform is the signal in the time domain which takes the form of the signal appearing in Figure 6:

$$p(r, z; t_j) = \mathfrak{F}^{-1}[p(r, z; \omega_i)] \quad (23)$$

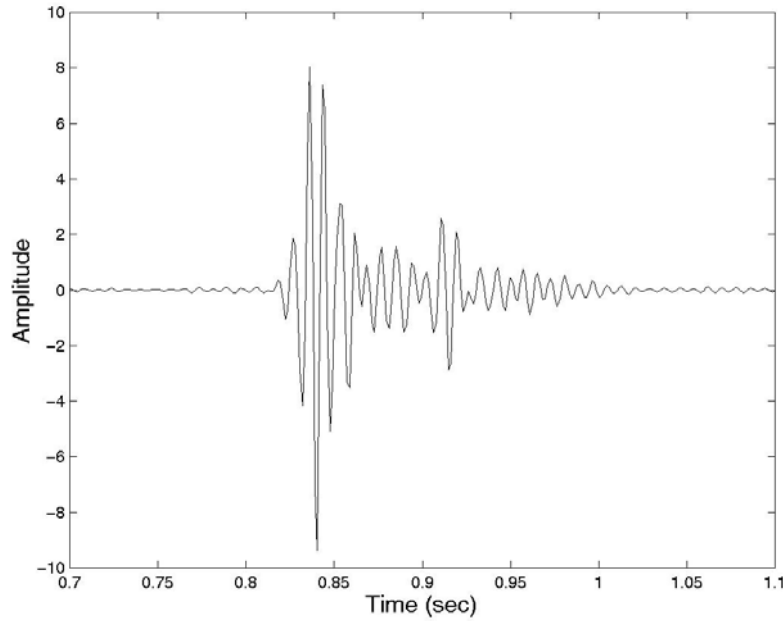


Figure 6. The simulated gaussian signal in the time domain  
Central frequency 115 Hz

Parameter	True value	Upper search bound	Lower search bound
Water depth $D$ (m)	115.3		
Sound speed at the surface $c_w(0)$ (m/sec)	1480	1470	1490
Sound speed at the water/bottom interface $c_w(D)$	1460	1440	1500
Source depth $z_0$ (m)	26.4		
Sediment thickness $h$ (m)	27.1		
Sediment sound speed $c_b(D)$	1516.2	1450	1550
Sediment sound speed $c_b(D+h)$	1573.2	1500	1700
Sediment density, $\rho_b$ (g/cm <sup>3</sup> )	1.538		
Subbottom sound speed $c_{sb}$ (m/sec)	1751.26		
Subbottom density $\rho_{sh}$ (g/cm <sup>3</sup> )	1.852		

*Table 1: Environmental parameters of the test environment.*

No noise has been added. It should be noted however, that as previously stated, noise is expected to have minimum effect on the identification of the modal peaks. Noise may change the amplitude of the peaks of the signal, and more peaks may appear, but the location of the modal arrivals is not changed.

Table 1 presents all the known and unknown parameters of the environment, together with the search bounds considered for the sound speed in the water and the compressional velocity in the sediment layer.

Before starting the inversion procedure it is interesting to perform a qualitative analysis of the signal as regards the possibility of separation of the modal packets. The analysis is performed for the effective frequency bandwidth of 50 Hz and it is presented in Figure 7 in the form of the group velocity dispersion curves.

A close examination of the dispersion curves show that modes 1 and 2 are difficult to resolve as the corresponding group velocities for the whole signal bandwidth are very close to each other. Also the high dispersion of the group velocity for modes greater than 10 and in the neighbourhood of the central frequency is an indication that the corresponding modal packets will not be very sharp.

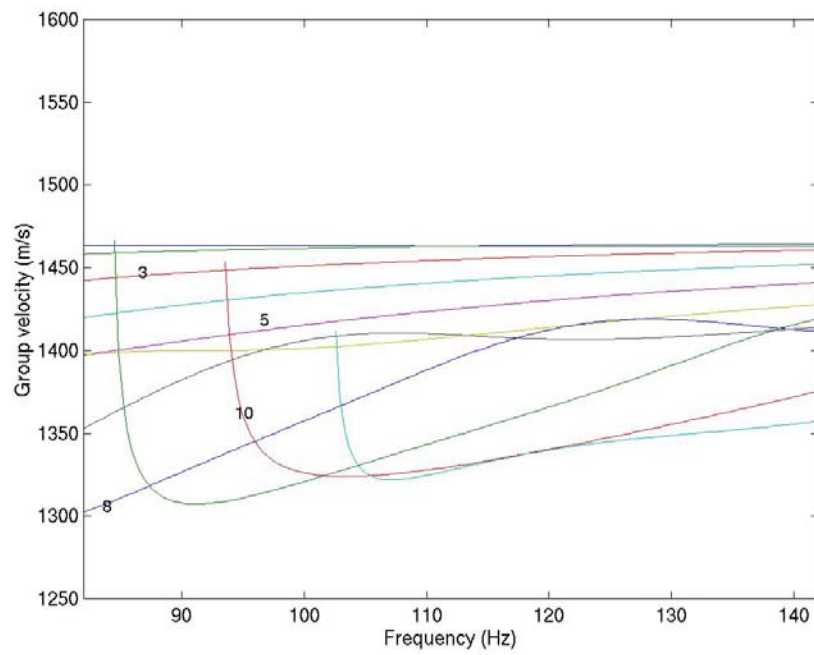


Figure 7. The dispersion curves

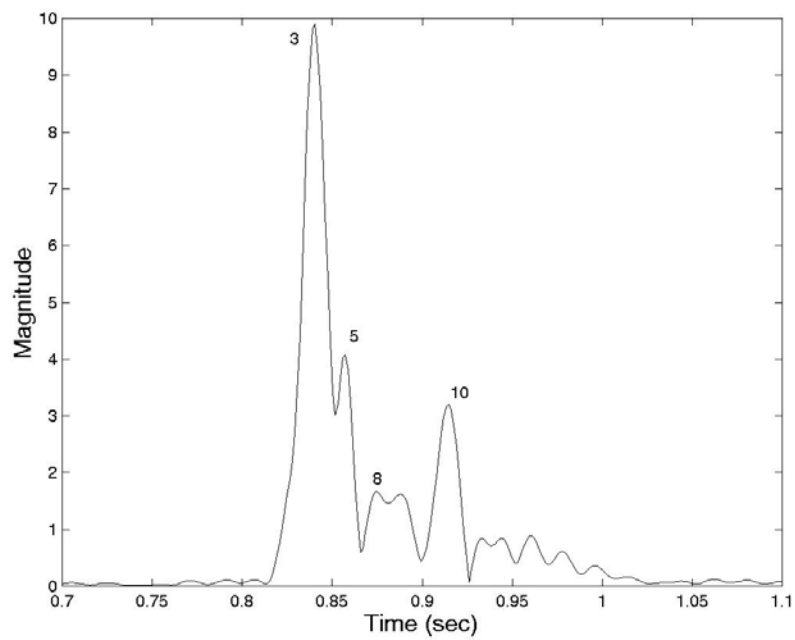


Figure 8. The arrival pattern of the simulated tomographic signal with central frequency 115 Hz

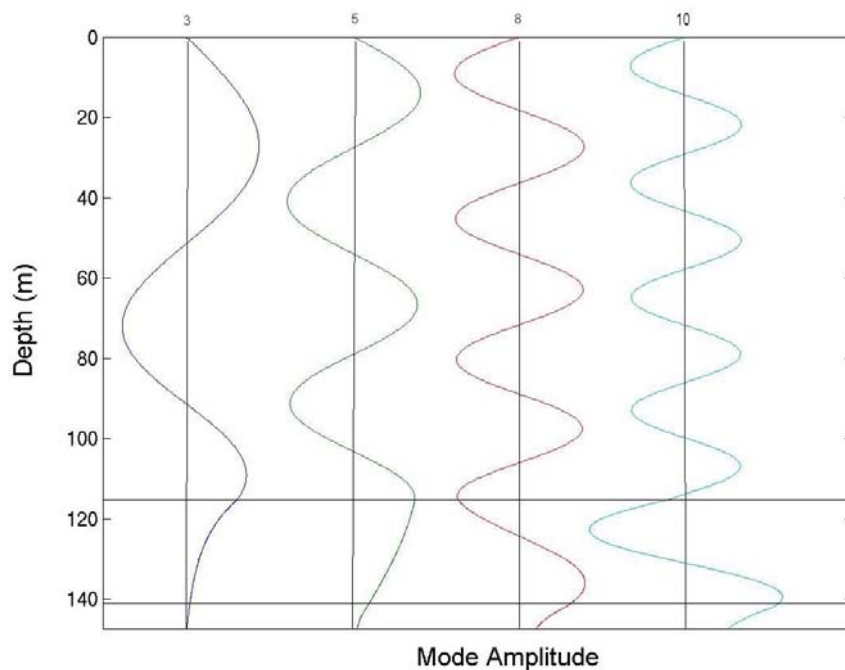


Figure 9. The eigenfunctions for the order of identified modal arrivals at the central frequency of 115 Hz.

The arrival pattern of the signal appears in Figure 8.

The figure shows the identified modal arrivals, using the known group velocities at the central frequency. It is noted that the identification at this stage was made possible here only because the actual environment is known. In realistic applications, the identification is a result of the inversion procedure as described above.

The eigenfunctions at the central frequency for the identified modes 3, 5, 8 and 10 are shown in Figure 9. It can be easily seen that there is enough penetration in the bottom for all these modes and therefore one might expect that bottom inversion is possible.

## 5.2 The inversion procedure for bottom recovery

We apply the inversion procedure separately for water and sediment sound speed recovery. In both cases a two-dimensional search space is defined on the basis of the search bounds appearing in Table 1. We divide the search space for the sound velocity of the upper part of the sediment in 25 segments and the same for the lower part in 50 segments, thus defining 1250 possible reference environments. Performing the identification for each one of the reference environments, we produce the contour plot of Figure 10, which shows the identification norm for the two dimensional search space.

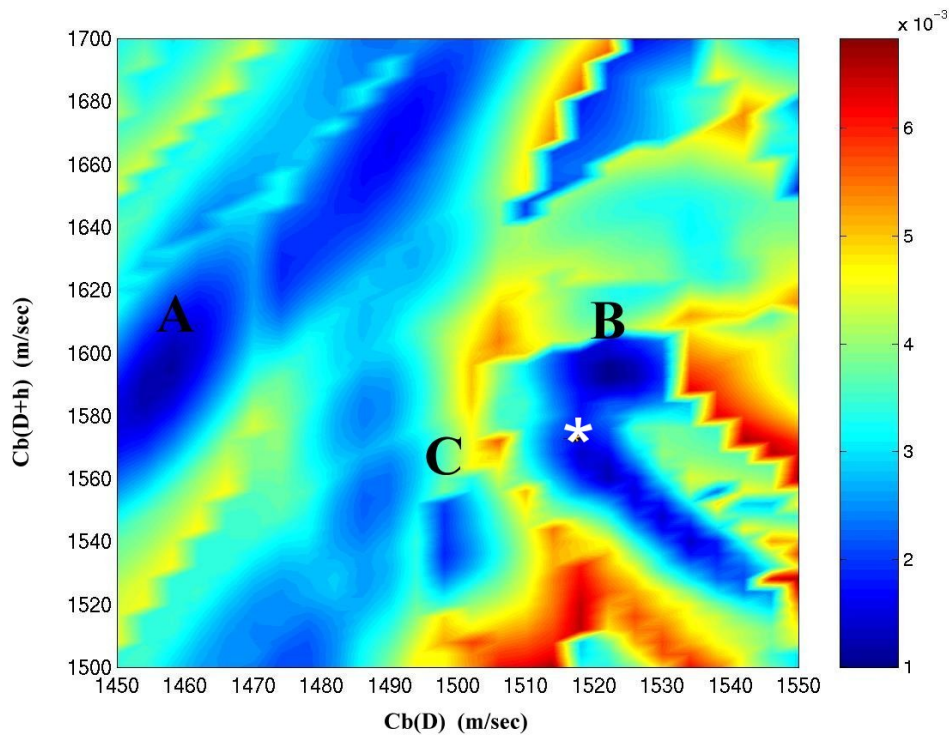


Figure 10. The identification norm using the signal corresponding to  $f_0=115$  Hz

It can be easily seen that the identification norm exhibits three significant areas of minimum norm. In Figure 10 the actual pair is also indicated by star and its location falls very close to the location of the minimum norm for two of the three areas. It is however away from the third area where another minimal norm is also shown.

Another qualitative analysis is made with the help of the Figure 11. The diagram presents the number of times a specific peak of the arrival pattern is identified as a modal arrival, and the corresponding order. For instance it is shown that mode No 3 is always identified in peak #1 of the arrival pattern. In most cases peak #2 is identified as modal arrival of order 5, in accordance with the actual identification presented before. Peak #3, however, is identified most times, as the mode of order 6, and this is not in accordance with the actual mode identification. This is an indication that the higher order modes are more sensitive to the identification process, and their location in the time domain varies substantially with varying sound speed value. However, it is confirmed that in the two areas of the minimum norm (Figure 10) close to the actual pair of the sound speed values, the identification corresponds to the correct orders of modes in the associated arrival pattern peaks.

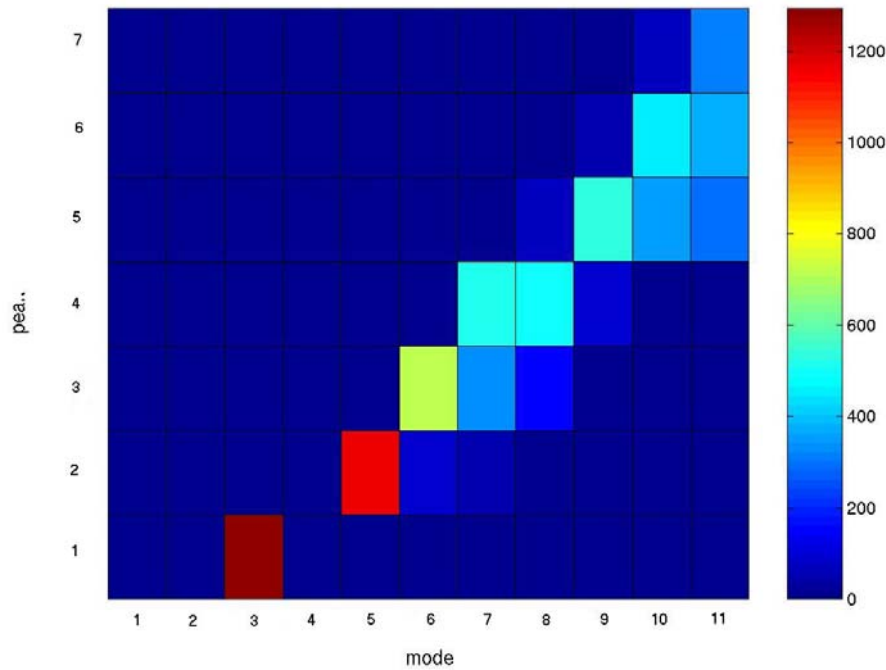


Figure 11 The statistics of the identified modal arrivals ( $f_0=115$  Hz)

### 5.3 The local search

In order to more closely approach the actual solution, we applied the local linear inversion algorithm starting from different node points of the three significant areas of minimum norm. The iterative inversion procedure in the area A did not converge. Convergence was ensured when the local inversion scheme was applied starting from nodal points of areas B and C. Starting from the pair corresponding to the local minimum of area C (indicated in Table 2 under Reference heading), we obtain after a few iterations the results appearing in the fourth column of Table 2. It can be easily seen that the results agree well compared with the actual pair indicated in the second column of the table despite the fact that area C is not the closest to the actual values.

Parameter	Actual	Reference environment after matching the modal peaks	Inverted after the linear process
$C_b(D)$ (m/sec)	1516.2	1506.1	1517.44
$C_b(D+h)$ (m/sec)	1573.2	1539.5	1569.84

Table 2. Inversion results using the hybrid approach for the recovery of the sound speed in the sediment layer.

The performance of the inversion algorithm was the same when applying the scheme with higher central frequencies. This is shown in Figures 12 and 13 presenting the arrival pattern and the identification norm when the central frequency is 150 Hz. Note that the identified modal arrivals are different than those in the case of 115 Hz central frequency.

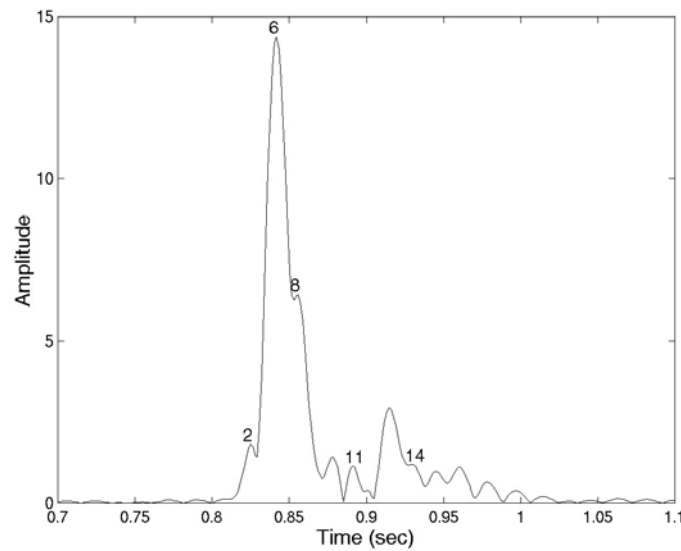


Figure 12. The arrival pattern of the signal with  $f_0 = 150 \text{ Hz}$

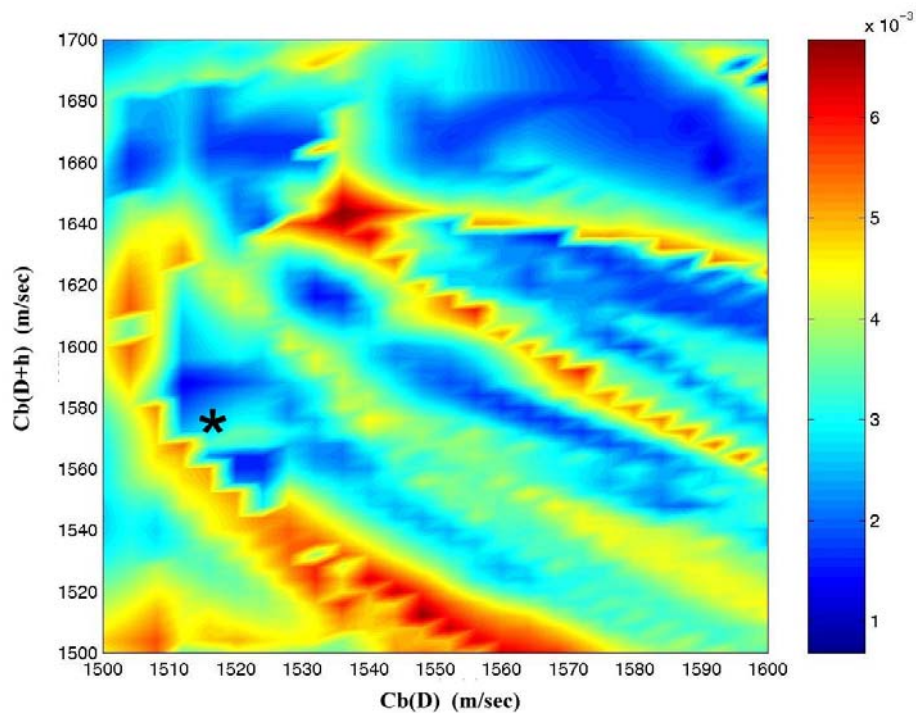


Figure 13. The identification norm using the signal with  $f_0 = 150 \text{ Hz}$ 

Parameter	Actual	Inverted (115 Hz)	Inverted (150 Hz)
$C_w(D)$	1516.2	1517.44	1517.47
$C_w(D+h)$	1573.2	1569.84	1573.98

Table 3 Inversion results when using the signal corresponding to central frequency  $f_0=150 \text{ Hz}$ , in comparison with inversion results using the signal corresponding to central frequency  $f_0=115 \text{ Hz}$ .

In this case more areas of minimal norms appear. However, the application of the linear inversion scheme though showed again that convergence is still ensured when starting from a reference environment close to the actual one determined by the matched-modal-peak approach.

#### 5.4 Inversion for the water column sound velocity

The inversion scheme was also applied for the recovery of the sound speed profile in the water column under the assumption that the bottom properties and water depth are known and fixed to the actual values. Using the same procedure and the search space shown in Table 1, with central frequency  $f_0=150 \text{ Hz}$ , the identification procedure is based on the arrival pattern shown in figure 12 and generates the identification norm contour plot of figure 14.

It is clearly seen that the significant areas of minimum norm are greatly reduced in this case. Two such areas are now present. The iterative procedure starting from the environment corresponding to the absolute minimum of the identification norm produces excellent results as shown in Table 4.

Parameter	Actual	Reference environment after matching the modal peaks	Inverted after the linear process
$C_w(0) \text{ (m/sec)}$	1480	1484	1480.95
$C_w(D) \text{ (m/sec)}$	1460	1455	1458.73

Table 4. Inversion results for the sound speed in the water column

The better performance of the matching process is due to the fact that the identified modes are rich in information on the water column structure. The identification process works much better than in the case of bottom geoacoustic inversion, and this is due to the fact that modal arrivals for the orders of the identified modes are more sensitive to changes in the water column than to changes in the sediment.



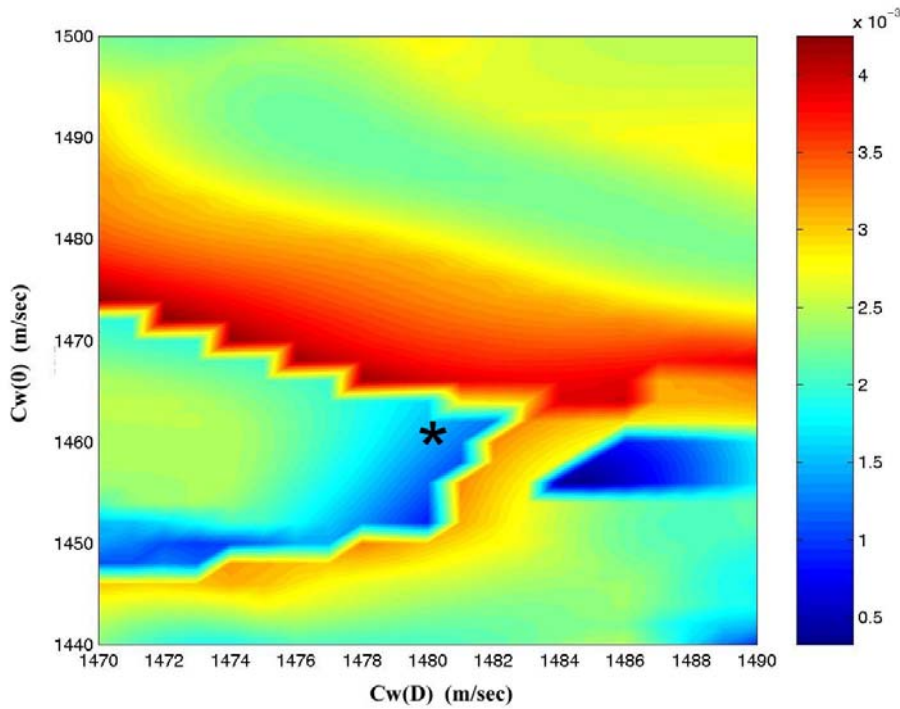


Figure 14. The identification norm for the recovery of the sound speed in water ( $f_0=150$  Hz)

## 6. Conclusions

The results presented here, show a satisfactory behaviour of the inversion toolbox for the recovery of the water column and bottom sound velocity in a range-dependent shallow water waveguide. It is recalled that a broad-band source has been considered and that the inversion was based on a hybrid approach incorporating a matching procedure for the modal arrivals of the arrival pattern of signal with a linear inversion scheme based on the reference environment(s) defined at the first stage.

It should be noted that the results presented here are referred to a matching procedure over a two dimensional search for both the water column and sediment sound speed recovery. The thickness and density of the sediment layer and the basement are considered known. From a first glance, these assumptions seem not to be realistic if we consider actual situations. However, sensitivity studies performed in the validation process of the inversion toolbox have shown that sub-bottom properties and sediment density variations do not have a significant influence in the variation of the corresponding sound field. They can, therefore, be excluded from the inversion process, at least for an initial estimate of the rest parameters. On the other hand it is important that the assumption of a reference environment close to the actual one can be relaxed and we consider realistic variations of the sound speed in the water column and the upper sediment layer only.

The sound velocity has been considered linearly varying in both media. Working with synthetic results, no noise has been considered. However, since we are dealing with significant peaks of the signal in the time domain only, it is expected that noise will have a small effect on the overall performance of the toolbox. This is due to the fact that the position of the modal peaks is not influenced very much by the noise, especially when an averaging process in the actually measured signals is adopted. This statement has been confirmed by real tomographic experiments of a similar configuration [24].

Another point of interest is that lower order modes contain less information about bottom structure compared to the higher order ones. Thus, it is expected that in order to get a reliable inversion for the bottom structure, it is important that higher order modes are identified as well. Following this remark, the inversion for both water and sediment sound speed profile could proceed in two stages, the first of which would lead to the recovery of the sound speed in water using lower order modes and the second would lead to the recovery of the compressional velocity in the sediment layer using higher order modes.

Future work includes the study of the influence that the location of the receiver has on the accuracy of the results. Moreover, exploitation of the measurements made at a vertical array of hydrophones is expected to improve the quality of the results. However this approach falls beyond the scope of our work, which is concentrated to a single receiver case.

Although results with synthetic data are promising, the actual validation of the toolbox can only be done after real data have been analysed. The authors also intend to extend the inversion algorithm to a multi-dimensional search space.

## Acknowledgments

We would like to express our thanks to Mrs Eirini Mavritsaki for her computational help in developing the modal identification scheme. We would also like to thank the reviewers of the paper for their critical remarks.

## References

1. S. Rajan, J.F. Lynch, and G.V. Frisk, "Perturbative inversion methods for obtaining bottom geoaoustic parameters in shallow water," *J.Acoust.Soc.Am.* **82** (1987) 998-1017.
2. E.C. Shang, "Ocean acoustic tomography based on adiabatic mode theory," *J.Acoust.Soc.Am.* **85** (1989) 1531-1537.
3. M. I Taroudakis and M.G. Markaki, "On the use of matched field processing and hybrid algorithms for vertical slice tomography," *J.Acoust.Soc.Am.*, **102** (1997) 885-895.

4. M.I. Taroudakis and J.S.Papadakis, "A modal inversion scheme for ocean acoustic tomography," *J. Comp. Acoustics*, **1**, (1993) 395-421.
5. F.B. Jensen, W.A.Kuperman, M.B.Porter, H.Schmidt *Computational Ocean Acoustics*, American Institute of Physics, New York 1994.
6. D.M.F. Chapman and D. Ellis: "The group velocity of normal modes", *J.Acoust. Soc.Am.* **74** (1983) 973-979.
7. W. Munk and C. Wunsch, "Ocean Acoustic Tomography: Rays and Modes," *Rev.Geoph. Space.Phys.* **21** (1983) 777-793.
8. C.T.Tindle, K.M. Guthrie, G.E.J. Bold, M.D.Johns, D. Jones, K.O.Dixon and T.G. Birdsall, "Measurements of the frequency dependence of normal modes," *J.Acoust.Soc.Am.* **64** (1978) 1178-1185.
9. W. Munk and C. Wunsch, "Ocean Acoustic Tomography: A scheme for large scale monitoring," *Deep Sea Res.* **26a**, (1979) 123-16.
10. E.C.Shang and Y.Y. Wang, "On the possibility of monitoring the El Niño by using modal ocean acoustic tomography" *J.Acoust.Soc.Am.* **91** (1992) 136-140.
11. M.I.Taroudakis, "A comparison of the modal-phase and modal-travel time approaches for ocean acoustic tomography" in *Proceedings of the 2nd European Conference on Underwater Acoustics*, edited by L.Bjørnø, pp. 1057-1062, 1994.
12. E.K. Skarsoulis, G.A. Athanassoulis and U. Send, "Ocean acoustic tomography based on peak arrivals," *J.Acoust.Soc.Am.* **100** (1996) 797-813.
13. G.A. Athanassoulis, J.S. Papadakis, E.K. Skarsoulis and M.I. Taroudakis, "A comparative study of modal and correlation arrival inversion in ocean acoustic tomography" in *Full Field Inversion Methods in Ocean and Seismic Acoustics* edited by O.Diachok, A Caiti, P. Gerstoft and H Schmidt, Kluwer Academic Publishers, 127-132, 1995.
14. E.K. Skarsoulis "An adaptive scheme for ocean acoustic tomography of large sound-speed variations" in *Proceedings of the 3<sup>rd</sup> European Conference on Underwater Acoustics*, edited by J.S.Papadakis, IACM/FORTH 803-808, 1996.
15. A.Tolstoy, *Matched Field Processing for Underwater Acoustics*, World Scientific, Singapore, 1993.
16. D.E.Goldberg, *Genetic Algorithms in Search Optimization and Machine Learning*, Addison\_wesley, Reading, MA, 1979
17. P.Gerstoft "Inversion of seismoacoustic data using genetic algorithms and a posteriori probability distributions", *J.Acoust. Soc. Am.* **95** (1994) 770-782.

18. M.I.Taroudakis and M.G.Makraki "Bottom Geoacoustic Inversion by "Broadband" matched-field processing" *J.Comput.Acoust.* **6** (1998) 167-183.
19. M.R.Fallat and S.E.Dosso "Geoacoustic Inversion for the Workshop '97. Benchmark cases using Simulated Annealing" *J.Comput.Acoust.* **6** (1998) 29-43, 1998.
20. M.K. Sen and P.L.Stoffa "Bayesian interference, Gibb's sampler and uncertainty estimation in geophysical inversion" *Geophys. Prospect* **44** (1996) 313-350.
21. A. Tolstoy "MFP Benchmark inversions via the Rigs method" *J.Comput.Acoust.* **6** (1998) 185-203.
22. M.I.Taroudakis, "Identifying modal arrivals in shallow water for bottom geoacoustic inversions", *J.Comput.Acoust.* **8** (2000) 307-324.
23. A.Tolstoy, N.R.Chapman and G. Brooke, "Workshop'97: Benchmarking for geoacoustic inversion in shallow water," *J.Comput.Acoust.* **6** (1998) 1-28.
24. U.Send et al. "Acoustic observations of heat content across the Mediterranean Sea," *Nature* **385** (1997) 615-617.